AMD-Vol. 196, Failure Mechanics in Advanced
Polymeric Composites
ASME 1994

THE 3D STRESS FIELD IN A LAMINATED COMPOSITE PLATE WITH A HOLE BASED ON AN h-r FINITE ELEMENT METHOD

Yong-Kyu Choi
Agency for Defense Development
Taejon, Korea

Efthymios S. Folias
Department of Mathematics
University of Utah
Salt Lake City, Utah

ABSTRACT

This paper deals with the 3D stress field in a laminated composite plate that has been weakened by the presence of a hole and has been subjected to a uniform displacement along the horizontal direction. The composite plate is made of transversely isotropic laminae, e.g. [0/90]. Particular emphasis is placed on the interlaminar stresses in the region adjacent to the hole where delamination is most likely to occur. For the analysis, a three-dimensional h-r adaptive finite element computer code, "HRHOLD3D", has been developed for the solution of elastic problems. The adaptive method developed searches for an optimum mesh and leads to more accurate results with a minimum number of nodes. The code is very efficient and runs on personal computers. Comparison with 3D analytical results for isotropic plates shows an excellent agreement thus substantiating its validity and its potential use. The analysis shows that the interlaminar normal stress is highly dependent on the plate thickness while the interlaminar tangential stress is very weakly dependent. Comparison of the delamination strength with available in the literature experimental data shows a very good agreement.

INTRODUCTION

Despite careful design, practically every structure contains stress concentrations due to holes. Bolt holes and rivet holes are necessary components for structural joints. It is not surprising, therefore, that the majority of service cracks nucleate in the vicinity of a hole. While the subject of stress concentrations is certainly familiar to engineers, the situation is significantly more complex in the case of high-performance laminated composite materials. The presence of a hole in the laminate introduces significant stress contributions in the third dimension which create a very complicated three-dimensional stress field in the vicinity of the hole. Moreover, this complex state of stress may depend on the stacking sequence of the laminate, the fiber orientation of each lamina as well as the material properties of the fiber and of the matrix. Ultimately, these stress concentrations form a primary source of damage initiation and property degradation, particularly in the presence of cyclic loading.

Delamination along the interface of two adjacent laminae has long been recognized as one of the most important failure modes in laminated composite structures. The growth of a delamination may result in a substantial reduction of strength and stiffness of the laminate. The identification, therefore, of such locations in a composite structure is of great interest to the designer. Experimental studies by Pipes et al. (1973) have shown that the delamination mode of failure is most likely to initiate at the free edges. As a result, several researchers have attempted to extend their 2D theories to such 3D problems with limited success. In particular, the derived results were either poor or were applicable only to certain regions. Alternatively, for 2D problems, analytical solutions are presently available in the literature (e.g. see Lekhnitskii 1963) which provide us with some insight into the stress field in the neighborhood of hole edges.

For this reason and particularly for complex structural geometries, researchers have turned to the use of the method of FEM. Several authors have studied the 3D problem of a composite plate but they have encountered computing difficulties due to memory. Consequently, as an alternative tool, they have frequently chosen a combination type of method, for example, a combination of a 2D CLT with a 3D FE method (Raju et. al. 1982) or a 2D FE with a 3D FE method (Lucking et. al. 1984) or a rezone method. Although experience tells us that far away from the hole the error is expected to be relatively small, the answer may still be affected due to error pollution. In general, areas which are far away from the free edge do not require as many elements for the stress-strain fields there are relatively simple. Computing difficulties, due to memory, however, may still be encountered because the regular pattern mesh requires the same number of matching nodes on each opposite side. Moreover, the mesh generation was based primarily on the analyst's previous experience and verification of the convergence of the solution was accomplished by comparing the results with corresponding results obtained from a remesh generation.

Recently, various methods of refinement, involving either the subdivision of elements (h-refinement) or the increase of the order of the polynomials defining the shape function (p-refinement), have been proposed. However, very little research has been done in order to extend and improve these adaptive methods for use in the FE analysis of composite structures. In this investigation, utilizing the mesh adjustment and refinement technique (which in the literature is referred to as the h-r adaptive method), the problem of a composite plate which has been weakened due to the presence of a circular hole is investigated and the 3D effect that the ratio of hole radius to plate thickness has on the overall stress field is examined.

FINITE ELEMENT FORMULATION

"HRHOLE" is the 3D adaptive displacement-formulated FE computer code which consists of the following three components (i) the conventional displacement formulated FE calculation, (ii) the error estimation, and (iii) the mesh size adjustment or refinement. The conventional displacement-formulated FEM component consists of three procedures: integration, assembling and matrix solving. This formulation, which is based on the displacements, has been used for various engineering applications because of its theoretical simplicity. The order of integration, however, is still retained as an argumentation. Equation (1) is the well known transformation equation from an isoparametric space to a 3D orthogonal space.

$$\begin{Bmatrix} \frac{\partial N_i}{\partial x_i} \\ \frac{\partial N_i}{\partial y_i} \\ \frac{\partial N_i}{\partial z_i} \end{Bmatrix} = J^{-1} \begin{Bmatrix} \frac{\partial N_i}{\partial \xi_i} \\ \frac{\partial N_i}{\partial \psi_i} \\ \frac{\partial N_i}{\partial \zeta_i} \end{Bmatrix}, \text{ where } J = \begin{Bmatrix} \frac{\partial x_i}{\partial \xi_i}, \frac{\partial y_i}{\partial \xi_i}, \frac{\partial z_i}{\partial \xi_i} \\ \frac{\partial x_i}{\partial \psi_i}, \frac{\partial y_i}{\partial \psi_i}, \frac{\partial z_i}{\partial \psi_i} \\ \frac{\partial x_i}{\partial \zeta_i}, \frac{\partial y_i}{\partial \zeta_i}, \frac{\partial z_i}{\partial \psi_i} \end{Bmatrix} \qquad (1)$$

In an isoparametric space, the order of the polynomial representing the strain components will be of one order lower than the degree of the displacement polynomial along the differentiated direction. The strain components in the other direction, however, still remain of the same order polynomial. Moreover, the elements are not always square in shapes. Some of the elements may be distorted due to the geometry of the structure which is being analyzed. Consequently, the Jacobian inverse shows a much more complicated state. Therefore, the order of the strain component is deduced to be equal to or greater than the order of the shape function . In the numerical analysis, the entire process is performed using the numerical values which are the so- called stationary values. Consequently, the decision regarding the selection of the number of sampling points is very important in determining these stationary values. Based on the above observations, the minimum order of integration must be used with great care, and it is for this reason that Bathe and Wilson (1976) recommended the normal or maximum order of Gaussian integration.

The number of integration order relates, not only to the integration error, but also to other factors such as the smoothing technique, the shape function of the stresses as well as the estimation of error. In order to obtain more reliable nodal data with limited calculations, smoothing techniques have been suggested by Hinton et. al. (1974). The basic idea of this technique is to minimize numerically the discontinuity of stresses by using the least squares method. In this investigation, we define two errors: a local error and a global error. The former is due to the integration order while the latter is due to the assumed shape function.

The error estimator that was used in this investigation was suggested first by Zienkiewicz and Zhu (1987). However, using the energy norm concept, the error estimator did not provide us with any directional information regarding refinements. For this reason, in this investigation the concept was modified so that it would be more suitable for the h-r method. It may also be noted that the residual error ,due to interpolation depends not only on the nodal position, but also on the distance that exists between nodes. Thus, the RMS-type error estimator based on the node, which provided the magnitude of error in addition to the refinement direction, was applied. Before applying the adaptive method , the availability of the error estimator was tested by using a uniform patterned mesh. By virtue of this test, the maximum integration method was shown to be the best method for (i) smoothing the stress profile and (ii) for providing reliable information regarding the magnitude of the error. The method was very effective, particularly for distorted elements. Using this error information, the adaptive process was performed. All of the adaptive processes were designed to have an automatic facility by implementing all of the logic to computer code. For the adaptive processes, the logics were set up and substantiated with existing in the literature 3D analytical solutions for isotropic plates (Folias, et. al. 1990).

NUMERICAL RESULTS

As a specific example, we consider the stress field of a composite plate consisting of four-ply laminates with a $[0/90]_S$ stacking sequences. Each ply is assumed to be homogeneous, linear elastic, orthotropic material that is defined by the properties (see Raja et. al. 1982):

E_{11} = 138 GPa ($20*10^6$ psi) $E_{22} = E_{33}$ = 14.5 GPa ($2.1*10^6$ psi)

$G_{12} = G_{23} = G_{31}$ = 5.86 GPa ($0.85*10^6$ psi)

$\nu_{12} = \nu_{13} = \nu_{23}$ = 0.21

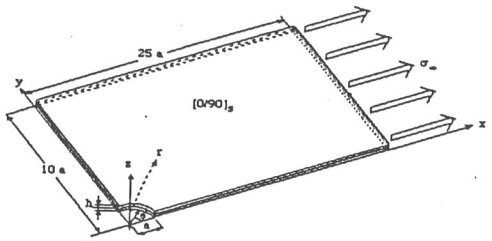

Figure 1. Laminate configuration, loading condition.

The subscripts 1, 2 and 3 denote, respectively, the longitudinal, transverse, and thickness directions of an individual ply. As it is shown in Figure 1, the geometric dimensions are a/w = 10, a/L = 25 and a/h = 1, 2, 3, 20 and 100. Because of the symmetry of the problem, only one-eighth of the laminate needs to be analyzed. As to loading, a uniform displacement, U_0, is applied in the x direction. This uniform displacement value was then set equal to 0.25h, that corresponds to the equivalent of 1% strain. Finally, in order to normalize the results, the gross-sectional stress σ_∞ corresponding to this deformation was evaluated. This stress value was obtained by adding first the stresses at the ends of the laminate and then dividing the result by the cross-sectional area. The resulting stress value is 72.5 MPa., which is lower by 3.8% than the corresponding value obtained from the CLT method. All stresses were subsequently normalized with respect to the stress σ_∞.

ADAPTIVE MESH PROCESS

The number of elements through the thickness (i.e. z-elements) was set at five because of the three zones, i. e. the free or interface boundary zone, the intermediate zone and the uniform zone. For example, the top material consists of five zones, which include the free boundary zone, the intermediate zone, the uniform zone, another intermediate zone and the interface zone.

There were two typical mesh models which resulted from the adaptive process in Figure 2. Mesh model "A" was generated for thin plates, for example a/h = 20 and 100, while mesh model "B" was generated for thick plates , for example a/h = 1, 2 and 4. Figure 3 illustrates the h-r adaptive process for generating Model "A." The final views of the 3D mesh shapes are presented in Figure 4. From the distorted mesh shapes, one deduces that a stress singularity may be present in the vicinity of the lamina interface. Similarly, in the case of thick plates, five zones were formed as a result of the interlaminar-singularity-effect and of the free z-surface effect. This phenomenon agrees with the previous assumption. The z-elements, far away from the boundary of the hole, appeared to be uniform in size. In view of the mesh configurations, one concludes that the boundary layer effect of the interlaminar is a localized phenomenon that prevails in a very small neighborhood adjacent to the hole boundary. This is in agreement with the analytical results obtained for isotropic plates (Folias 1988) as well as for transversely isotropic plates (Folias 1992).

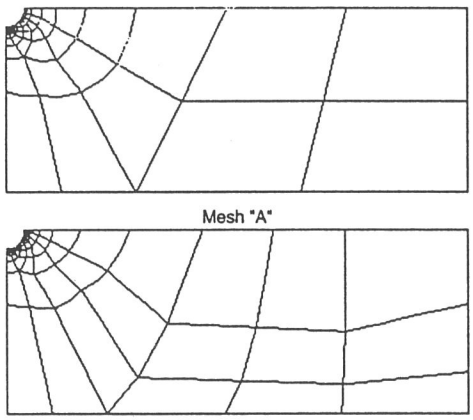

Figure 2. The final mesh configurations.

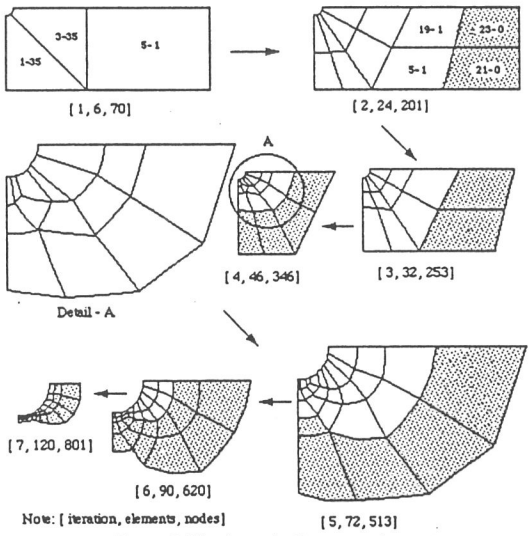

Figure 3. The h-r adaptive procedure.

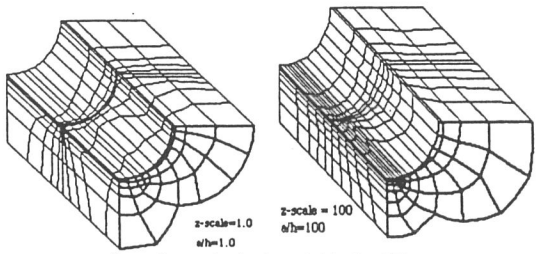

Figure 4. 3-D views of final mesh configurations, a) a/h=1 and b) a/h=100.

RESULTS AND DISCUSSION

Numerically, at a lamina interfacial node, four stress values exist for every stress component, i.e. the S-stress and the D-stress from each ply. When all four stresses values converged to the same value, the iterative calculation process was then considered to be complete. The results were subsequently plotted with respect to dimensionless geometrical variables (i.e., r/a, z/h, z/a, a/h). Finally, in order to investigate the effect of thickness on the stress distribution, stress profiles for various a/h ratios were plotted in the same figure.

Hoop Stress, $\sigma_{\theta\theta}$.

In the case of a plate with a ratio of a/h = 20 (see Figure 5.a) the present values are in good agreement with the 2-D CLT results, as well as with Raju and Crews' results (1982). The reader may also note (see Fig. 5.b) that the hoop stress depends on the plate thickness.

Figure 6 illustrates the hoop stress profiles as a function of the thickness for a/h = 20 and a/h = 1. As expected, the hoop stresses change rather abruptly as one approaches the interface. These sudden changes begin at z/h=1.12 ,for a/h=20, and at z/h=1.06, for a/h=1, and are due to the presence of the stress singularity which prevails in such neighborhoods.

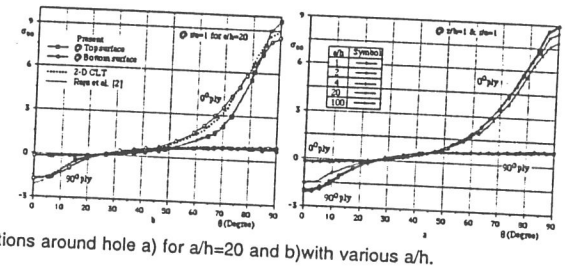

Figure 5. $\sigma_{\theta\theta}$ distributions around hole a) for a/h=20 and b)with various a/h.

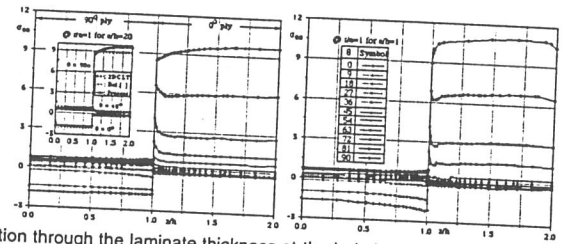

Figure 6. $\sigma_{\theta\theta}$ distribution through the laminate thickness at the hole boundary a)a/h=20 and b) a/h=1.

Interlamina Shear Stress for Radial Direction, s_{rz}.

Along the hole boundary, the stress s_{rz} should be zero if it is to satisfy the free boundary condition. Figure 7 shows the interlaminar stress distribution of s_{rz} through the radial direction for a plate with a/h = 20. As may be noted, the interlaminar stress s_{rz} increases to a maximum value, located at approximately r/a = 1.06, and then tends to the stress free condition. The maximum stress value occurred at $q = 63^{o}$. These numerical results did not perfectly satisfy the stress free condition at the hole boundary. The apparent discrepancy is most likely due to the presence of the interlaminar stress singularity at the hole boundary.

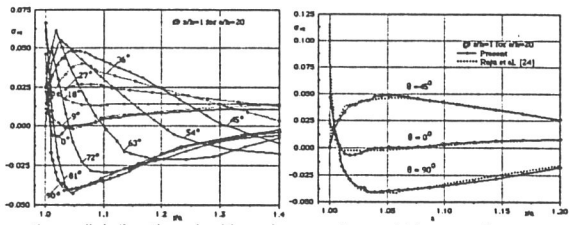

Figure 7. s_{rz} profile along the radial direction a) with various angles and b) comparison.

Interlamina Normal Stress, s_{zz}.

Figure 8 shows the interlamina normal stress along the hole boundary. However, discontinuities between the 0^o ply and the 90^o ply still exist from q = 60^o to q = 90^o. Such discontinuities, at the ply interface , have also been observed and reported by other authors (Raju et. al. 1982, Ericson et. al. 1984). Ericson et al. (1984) theorized that these discontinuities were due to the low accuracy in the out-of-plane stresses which were small in relation to the in-plane stresses, particularly at q = 90^o, where a large in-plane stress concentration occurs at the edge of the hole. The error estimator based on the energy norm can detect only the magnitude of the error, but not its origin. Figure 9 shows the stress profiles through the thickness direction. The present results are in good agreement with the results obtained by Raju and Crews except in the neighborhood of the interface region, which is approximately 3% in length of each ply thickness. The present results show the stress s_{zz} to attain its maximum within this region, while the results of Raju and Crews show the maximum s_{zz} to be at the ply interface. The authors believe that the interlamina normal stress should be continuous through the thickness even though this behavior is singular. At q = 90^o, even though a small discontinuity occurred in the present results, the trend was toward continuity, whereas the result of Raju and Crews revealed a divergent trend, even though the maximum value in their result was 100 % larger than the present value. As shown in Figure 10, the interlamina normal stresses increased/decreased slowly from a zero stress value , near (r-a) / h = 2.0, to their maximum values along the radial direction and then increased with a very steep gradient to the value at the hole boundary with their directional sign changed. The location of the maximum value occurred at (r-a) / h = 0.08. As we have previously noted, the interlaminar normal stress s_{zz} displayed, locally, a boundary layer type of behavior whereby it changes abruptly from tension to compression. The interlaminar stress s_{zz} also varied with thickness.

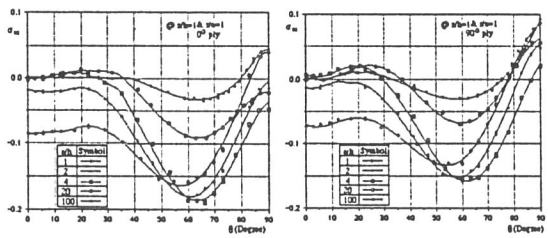

Figure 8. s_{zz} along the hole boundary with various ratios (a/h) at a) 0^o ply, b) 90^o ply .

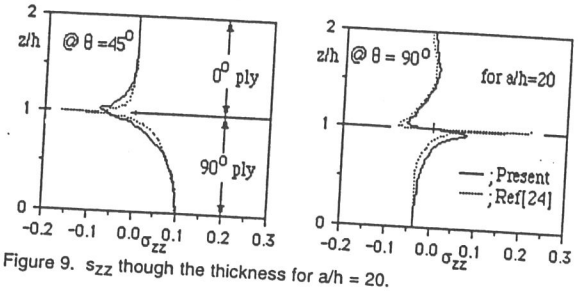

Figure 9. s_{zz} though the thickness for a/h = 20.

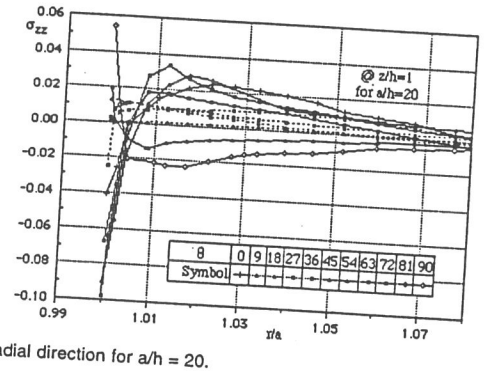

Figure 10. s_{zz} through the radial direction for a/h = 20.

Interlamina Shear Stress, s_{qz}.

The interlaminar stress s_{qz} is the largest of the three interlaminar stresses. Figure 11a shows the convergence of the interlaminar s_{qz} stress as a function of the number of iterations and Figure 11b shows its variation through the thickness. Moreover, as shown in Figure 12, the interlaminar stress s_{qz} exhibits a very weak dependence on the thickness parameter, a result that is in contradiction with that obtained by Lucking et al. (1984).

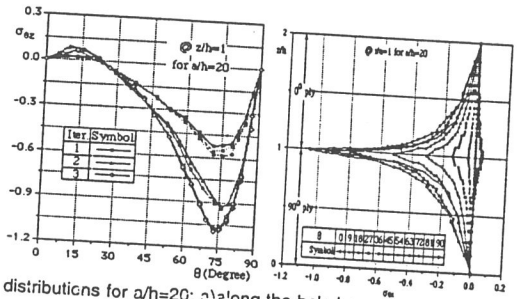

Figure 11. interlamina s_{qz} distributions for a/h=20: a)along the hole boundary and b) through the thickness.

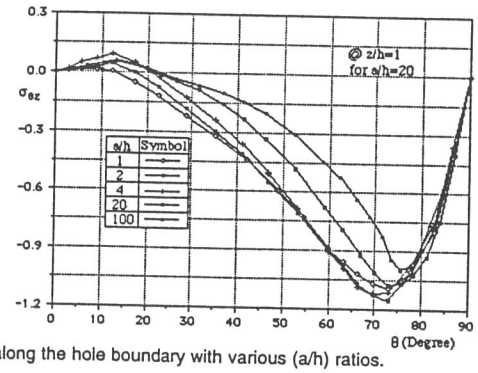

Figure 12. Interlamina s_{qz} along the hole boundary with various (a/h) ratios.

More specifically, their result shows the interlaminar stress s_{qz} to decrease as the ratio of a/h increases. This discrepancy is due to the fact that in their analysis a uniform size of z-elements was assumed. In the case of a uniform mesh model with a fixed number of z-elements, the actual size of z-element becomes larger when the ratio of a/h decreases. This type of mesh does not detect the singular characteristics, particularly in the case of thick plates, where the stress s_{qz} profiles exhibit very steep gradients in the vicinity of the hole boundary. These gradients were found to depend on the ratio of a/h.

DELAMINATION STRENGTH ANALYSIS

As it was previously noted, in the vicinity of the interface the interlaminar stresses exhibited a local boundary layer type of behavior with stress s_{qz} being the dominant of the four. It may also be noted (see Figure 13) that s_{qz} attains its maximum value at the hole boundary and that this value is approximately independent of the ratio a/h. Alternatively, along the radial direction, the gradient of the interlaminar stress s_{qz} varies with the ratio of a/h .

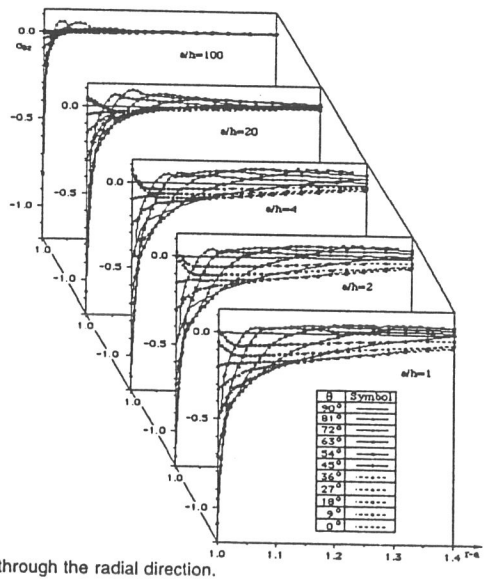

Figure 13. Interlamina s_{qz} through the radial direction.

As a practical matter, the final objective of this stress analysis is to assess the structural integrity of a structure against failure due to delamination. For this reason, two criteria immediately come to mind: (i) a point stress criterion and (ii) an average stress criterion.

In the case of a straight free edge, Wang and Choi (1982) have shown , analytically, that a weak stress singularity prevails at the free edge. Similarly, for curved free edges, Folias (1992) has shown, analytically, that a weak stress singularity is also present but in this case the singularity strength is a function of the position. angle q. The presence of a singularity will render a point stress criterion meaningless. On the other hand, the integral of the singular stress over a finite area will be finite. For this reason, the average stress criterion proposed by Kim and Soni (1984) has been recognized as more appropriate. In their paper , the average stress was defined as:

$$\overline{\sigma}_{ij} = \frac{1}{x_{avg}} \int_0^{x_{avg}} \sigma_{ij}(x)\ dx \qquad (2)$$

where x_{avg} ; average dimension is to be determined experimentally.

However, one strength parameter alone cannot properly predict the expected initiation stress of the different cases of interlaminar normal and shear stresses. In response to this Kim and Soni later introduced a criterion of the form:

$$F_{zz}\,\overline{\sigma}_z^2 + F_{tt}\,\overline{\sigma}_{xz}^2 + F_{uu}\,\overline{\sigma}_{yz}^2 + F_z\,\overline{\sigma}_z = 1 \qquad (3)$$

For the specific composite material which we have considered, the stress s_{qz} was the governing stress because the sum of the other two stresses was always less than 0.05. Thus, equation (3) reduces to the original equation, i.e., equation (2). If $\sigma_{ij}(x)$ is next normalized with respect to (rc-a), equation (2) may be expressed as:

$$\overline{\sigma}_{ij} = \frac{x_{avg}}{(\overline{x}_{rc})^2} \int_0^{\overline{x}_{rc}} F(\xi)\, d\xi$$

$$= \frac{x_{avg}}{(\overline{x}_{rc})^2} \left(G(0) - G(\overline{x}_{rc})\right)$$

$$= \frac{A_0}{(\overline{x}_{rc})^2} \left(1 - \frac{G(\overline{x}_{rc})}{G(0)}\right) \qquad (4)$$

where

$$G(x) = -\int F(x)dx, \text{ and } \overline{x}_{rc} = \frac{x_{avg}}{(r_c - a)}. \qquad (5a), (5b)$$

From equation (4), one can now see that the average stress depends only on the characteristic length $r_c(h)$, because x_{avg} is a material constant. If we next expand the stress distribution function F, as a Nth order of the polynomial, the delamination stress depends on $\overline{x}_{rc}$:

$$\overline{\sigma}_{ij}(h) = \sum_{i=-2}^{N-2} C_i \left(\overline{x}_{rc}(h)\right)^i, \text{ where } 0 < \overline{x}_{rc} < 1 \qquad (6)$$

For a linear function F, equation (6) becomes

$$\overline{\sigma}_{ij}(h) = \frac{(r_c(h) - a)^2}{C_0} - C_1 \qquad (7)$$

In order to investigate the thickness effect of the delamination strength, we define the characteristic distance as the distance from the hole boundary up to the location where s_{qz} reaches the value of $\pm 0.05\sigma_{\infty}$. Because the interlaminar s_{qz} stress profiles change with respect to the angle q, the characteristic distances also change. During this investigation, we were concerned primarily with the effect which thickness has on the delamination strength and not as much as on the location of the initial delamination. Thus, we used the average of s_{qz} to evaluate the characteristic length rc for the plates, as listed in Table 1. The material strength is constant. Therefore, the delamination strength of the plate has the reverse relationship of the interlaminar stress. The characteristic lengths a/(rc - a) are plotted in Figure 14 as a function of the ratio a/h.

Table 1. Characteristic length with various ratios of a/h.

a/h	100	20	4	2	1
(rc - a)/a	0.15	0.3	0.75	0.9	1.0
(rc - a)/h	15.0	6.0	3.0	1.8	1.0

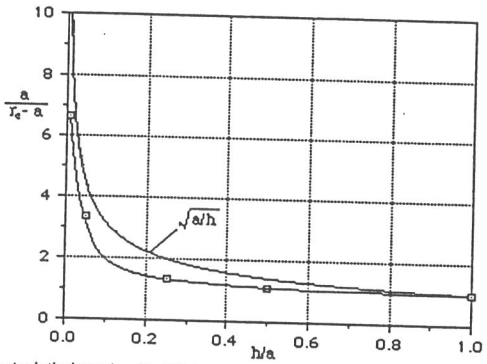

Figure 14. Normalized characteristic length with thickness.

The resulted delamination initiation strength is similar to that obtained experimentally for plates with straight edges by Brewer and Lagace (1988). Brewer and Lagace noted that the actual data of the delamination initiation stress appeared to decay more slowly than that of the strain energy release rate approach which predicts a decay that is proportional to the inverse of the square root of the ply thickness.

CONCLUSIONS

The thickness effect of a composite plate that has been weakened with a circular hole has been investigated using a 3D h-r adaptive FE computer code, "HRHOL3D." The interlaminar stress profiles, along the three directions, were presented and compared with previous results (Raju et. al. 1982, Lucking et. al. 1984). In general, the present results are in good agreement with those of Raju and Crews. The circumferencial stress was also in good agreement with the 2-D CLT exact solution. For the interlaminar normal and shear stresses, differences between the present results and those of Raju and Crews occurred only near the interface, i.e. in a region consisting of about 3% of each ply thickness. The analysis shows the interlaminar normal stress to depend on the plate thickness, however the interlaminar shear stress did not have any appreciable thickness dependency. The

thickness effect on the delamination strength has also been investigated, and the results were found to be in good agreement with the experimental results obtained by Brewer and Lagace (1988).

ACKNOWLEDGEMENTS

This work was supported in part by a research fellowship from ADD of Korea and in part by AFOSR under the direction of Dr. Walter Jones. The authors are grateful for this support.

REFERENCES

Bathe, K.J. and Wilson, E.L., 1976, Numerical Method in Finite Element Analysis, Prentice-Hall, Englewood Cliffs, NJ.

Brewer, J.C. and Lagace, P.A., 1988, "Quadratic Stress Criterion for Initiation of Delamination," Journal of Composite Materials, Vol. 22, pp. 1141-1155.

Ericson, K., Persson, M., Carlsson, L. and Gustavsson, A., 1984, "On the Prediction of the Initiation of Delamination in a [0/90]s Laminate with a Circular Hole," Journal of Composite Materials, Vol. 18, pp. 495-506.

Folias, E.S., 1992, "Boundary Layer Effects of Interlaminar Stresses Adjacent to A Hole in A Laminated Composite Plate," Int. J. Solids and Structures, Vol. 29, No 2, pp. 171-186.

Folias, E.S., 1988, " On the Interlaminar Stresses of a Composite Plate Around the Neighborhood of a Hole" , Int. J. Solids and Structures Vol. 25 (10), pp. 1193-1200.

Hinton, E. and Campbell, J.S., 1974, "Local and Global Smoothing of Discontinuous Finite Element Functions Using a Least Squares Method," Int. J. Numer. Meth. Eng., Vol. 8, pp. 461-480.

Kim, R.Y. and Soni, B.R., 1984, "Experimental and Analytical Studies on the Onset of Delamination in Laminated Composite," Journal of Composite Materials, Vol. 18, pp. 70-80.

Lekhnitskii, S.G., 1963, Theory of Elasticity of an Aniso-tropic Body, Mir Publishers, Moscow.

Lucking, W.E., Hoa, S.V. and Sankar, T.S., 1984, "The Effect of Geometry on Interlaminar Stresses of [0/90]s Composite Laminates with Circular Holes," Journal of Composite Materials, Vol. 17, pp. 188-198.

Raju, I.S. and Crews, Jr., J.H., 1982, "Three-Dimensional Analysis of[0/90]s and[90/0]s, Laminates with A Circular Hole," NASA-TM-83300.

Wang, S.S. and Choi, I., 1982, "Boundary-Layer Effects in Composite Laminates": Part 1-Free Edge Stress Singularities. Part II-Free Edge Stress Solutions and Basic Characteristics, Journal of Applied Mechanics, Vol. 49, pp. 541-560.

Zienkiewicz, O.C. and Zhu, J. Z., 1987, "A Simple Error Estimator and Adaptive Procedure for Practical Engineering Analysis," Int. J. Numer. Meth. Eng., Vol. 24, pp. 337-357.